Author(s): Ritch, Jamie; Chivers, Tristram; Eisler, Dana; Tuononen, Heikki

Title: Experimental and Theoretical Investigations of Structural Isomers of Dichalcogenoimidodiphosphinate Dimers: Dichalcogenides or Spirocyclic Contact Ion Pairs?

Year: 2007

Version:

Please cite the original version:

Ritch, J., Chivers, T., Eisler, D., & Tuononen, H. (2007). Experimental and Theoretical Investigations of Structural Isomers of Dichalcogenoimidodiphosphinate Dimers: Dichalcogenides or Spirocyclic Contact Ion Pairs?. Chemistry - A European Journal, 13(16), 4643-4653. https://doi.org/10.1002/chem.200700001

Experimental and Theoretical Investigations of Structural Isomers of Dichalcogenoimidodiphosphinate Dimers: Dichalcogenides or Spirocyclic Contact Ion Pairs?

Jamie S. Ritch,[a] *Tristram Chivers,**[a] *Dana J. Eisler,*[a] *and Heikki M. Tuononen*[b]

[a] J. S. Ritch, Prof. T. Chivers,* Dr. D. J. Eisler
Department of Chemistry
University of Calgary
Calgary, AB T2N 1N4 (Canada)
Fax: (+1) 403-289-9488
E-mail: chivers@ucalgary.ca

[b] Dr H. M. Tuononen
Department of Chemistry
University of Jyväskylä
P.O. Box 35, 40014 Jyväskylä (Finland)

Abstract

A synthetic protocol for the *tert*-butyl substituted dichalcogenoimidodiphosphinates [(tmeda)Na((EP*t*Bu$_2$)$_2$N)] (**3a**, E = S; **3b**, E = Se; **3c**, E = Te) has been developed. The one-electron oxidation of the sodium complexes [(tmeda)Na((EPR$_2$)$_2$N)] with iodine produces a series of neutral dimers (EPR$_2$NPR$_2$E-)$_2$ (**4b**, E = Se, R = *i*Pr; **4c**, E = Te, R = *i*Pr; **5a**, E = S, R = *t*Bu; **5b**, E = Se, R = *t*Bu; **5c**, E = Te, R = *t*Bu). Attempts to prepare **4a** (E = S, R = *i*Pr) in a similar manner produced a mixture including HN(SP*i*Pr$_2$). Compounds **4b**, **4c** and **5a-c** were characterized by multinuclear NMR spectra and by X-ray crystallography, which revealed two alternative structures for these dimeric molecules. The derivatives **4b**, **4c**, **5a** and **5b** exhibit acyclic structures with a central chalcogen–chalcogen linkage that is elongated by ca. 2% (E = S), ca. 6% (E = Se) and ca. 8% (E = Te) compared to typical single-bond values. By contrast, **5c** adopts an unique spirocyclic contact ion pair structure in which a [(TeP*t*Bu$_2$)$_2$N]$^-$ anion is *Te*,*Te'*-chelated to an incipient [(TeP*t*Bu$_2$)$_2$N]$^+$ cyclic cation. DFT calculations of the relative energies of the two structural isomers indicate a trend towards increasing stability for the contact ion pair relative to the corresponding dichalcogenide on going from S to Se to Te

for both the *iso*-propyl and *tert*-butyl series. The two-electron oxidation of [(tmeda)Na((EP*t*Bu$_2$)$_2$N)] (E = S, Te) with iodine produced the salts [(EP*t*Bu$_2$)$_2$N]$^+$ X$^-$ (**7a**, E = S, X = I$_3$; **7b**, E = Se, X = I; **7c**, E = Te, X = I), which were characterized by X-ray crystallography. Compound **7a** exists as a monomeric, ion-separated complex with [d(S-S) = 2.084(2) Å]; **7b** and **7c** are dimeric [d(Se-Se) = 2.502(1) Å; d(Te-Te) = 2.884(1) Å].

Keywords: chalcogens, dimerization, electronic structure, phosphorus, structural isomers

Introduction

The chemistry of dichalcogenoimidodiphosphinate ligands (**1**, E = O, S, Se) has been of keen interest in recent years.[1] These bidentate anions possess a flexible inorganic backbone compared to their organic counterpart, the β-diketonate ligand, which has a planar framework as imposed by the array of sp^2-hybridized carbon and oxygen atoms in the ligand framework. In addition, the ligands **1** have tunable electronic properties due to the variability of the substituents on the phosphorus atoms. Metal complexes of **1** (E = Se, R = *i*Pr) have recently been investigated as single-source precursors to semiconducting thin films of binary main-group metal selenides[2] and CdSe quantum dots[3] by the group of O'Brien. As well, ligands of the type **1** have been used to synthesize structurally rare square-planar complexes of Sn^{II} and Se^{II}.[4]

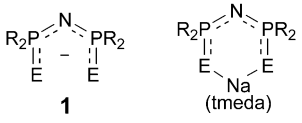

	E	R
2a:	S,	*i*Pr
2b:	Se,	*i*Pr
2c:	Te,	*i*Pr
3a:	S,	*t*Bu
3b:	Se,	*t*Bu
3c:	Te,	*t*Bu

By contrast to the extensive studies of the ligands **1** (E = O, S, Se), investigations of the chemistry of tellurium-containing analogues are relatively recent. In 2002 we reported the first synthesis of such a ligand, **1** (E = Te, R = Ph), which was isolated as the TMEDA-solvated

sodium salt.[5] The availability of this reagent, and, especially, the *iso*-propyl derivative **2c** has facilitated the development of the coordination chemistry of these tellurium-centred ligands. The syntheses of homoleptic complexes of group 12 and 15 metals,[6] as well as uranium and lanthanide complexes,[7] have been reported. Attempts to make homoleptic group 13 complexes resulted in an interesting tellurium-transfer reaction to give Ga_2Te_2 and In_3Te_3 rings.[8] These complexes have been shown to be suitable single-source precursors for the generation of pure thin films of certain metal tellurides, e.g. CdTe[9] In_2Te_3,[10] as well as Sb_2Te_3 nanoplates,[11] materials that are of interest for use in optoelectronic or thermoelectric devices.

A fascinating aspect of our investigations of the reactions of **2c** was the formation of the dimer **4c** via the one-electron oxidation with iodine [Eq. (1)].[12] A striking feature of the ditelluride **4c** is the long Te–Te bond (2.946(1) Å).[13] Thus, it can be viewed as two weakly associated tellurium-centred radicals, $[TeP\textit{i}Pr_2NP\textit{i}Pr_2Te]^{\bullet}$. DFT calculations[12] for the model system (R = Me) provide a Te–Te bond order that is significantly less than one; the calculated heat of dimerization is -80 kJ mol^{-1} compared to

a bond dissociation energy of 137 kJ mol^{-1} for PhTe–TePh determined by thermochemical methods.[14]

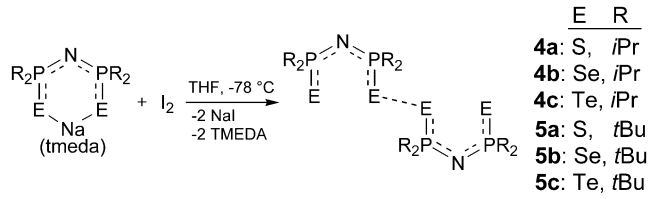

(1)

The discovery of **4c** represents a new aspect of the chemistry of dichalcogenoimidodiphosphinate ligands, whose redox behaviour has not been investigated in a systematic manner. In order to determine whether this type of redox transformation is a general phenomenon for this well-studied class of inorganic ligands, we have now addressed the influence of a change in (a) the chalcogen and (b) the substituents on phosphorus on the outcome of the one-electron oxidation of the corresponding anions in the sodium complexes **2a-c** and **3a-c** with iodine.[15] Syntheses have been devised for the *tert*-butyl-substituted reagents **3a-c**, which are new members of the family of dichalcogenoimidodiphosphinate ligands. Unexpectedly, the experimental work revealed the existence of a structural isomer for dimers of the type $(EPR_2NPR_2E-)_2$ (E = S, Se, Te). The relative energies of these two structural isomers, as a function of the chalcogen and the R group, were probed by DFT calculations. The synthesis and structures of the salts $[(EPtBu_2)_2N]^+ X^-$ (**7a**, E = S, X = I_3; **7b**, E = Se, X = I; **7c**, E

= Te X = I), obtained by the two-electron oxidation of **3a-c** with iodine, are also reported. Compound **7a** contains the previously unknown cationic ring system $[NP_2S_2]^+$.

Results and Discussion

Synthesis of 3a-c. The prediction of a longer Te–Te bond in $(TeP\textit{t}Bu_2NP\textit{t}Bu_2Te–)_2$ (**5c**) than that in the *iso*-propyl analogue **4c** by DFT calculations provided an incentive for the development of a synthesis of the *tert*-butyl-substituted reagent **3c.** The congeneric reagents **3a** and **3b** were also prepared for comparison of their behaviour upon one- and two-electron oxidations with that of **3c.** A variety of butyl-substituted ligands of the type $R_2P(S)NHP(S)R'_2$ (R, R' = *n*Bu, *i*Bu, *s*Bu) have been reported.[16,17] However, the synthesis of the symmetrical compound $HN(P\textit{t}Bu_2)_2$ has only been briefly mentioned in the literature; it was obtained in 50 % yield by the reaction of $\textit{t}Bu_2PNHM$ (M = unspecified alkali metal) with $\textit{t}Bu_2PCl$ at 100 °C for 2 h, and was only characterized by the ^{31}P NMR chemical shift (δ 83.0).[18]

The usual method for the preparation of symmetrical derivatives of the type **I** is the condensation of R_2PCl with $HN(SiMe_3)_2$, via elimination of Me_3SiCl.[1a] However, $\textit{t}Bu_2PCl$ fails to react in this manner, even under forcing

conditions (boiling xylenes),[19a] and so another synthetic approach was required.

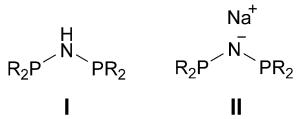

I II

The formation of a P–N–P framework via auto-condensation of a P–NH_2 moiety has long been known. For instance, several early studies on diorganophosphinyl amides, $R_2P(E)NH_2$, revealed that these compounds self-condense to form the corresponding dichalcogenoimidodiphosphinates, $HN(EPR_2)_2$, and ammonia upon thermolysis.[19b,c] In the light of these reports we pursued the synthesis of **I-*t*Bu** by a self-condensation route [Eq. (2)].

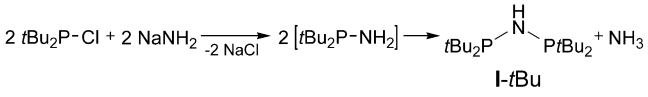

I-*t*Bu (2)

The reaction of tBu$_2$PCl with $NaNH_2$ in a 1:1 molar ratio in THF gives the desired product as a colourless crystalline solid in moderate yield (52 %). Monitoring the reaction by ^{31}P NMR revealed the formation of tBu$_2$PNH_2[18] as an intermediate and indicated that **I-*t*Bu** is present as the major species in the reaction mixture after stirring for 3 h at room temperature. However, complete conversion of the starting material can be achieved by heating to 60 °C for 2

h. The product is readily soluble in organic solvents and can be recrystallized from hexane.

The ^{31}P NMR spectrum ([D_6]benzene) of **I-*t*Bu** at room temperature consists of the expected sharp singlet at δ 83.0, together with two mutually coupled doublets at δ 87.5, 40.0 ($^2J_{P,P}$ = 43 Hz), which represent ca. 30 % of the total signal. In the proton-coupled ^{31}P NMR spectrum the resonance at δ 40.0 appears as a broad doublet with a coupling constant indicative of a P–H bond ($^1J_{P,H}$ = 390 Hz). The low resolution electron-impact mass spectrum of the product showed only the expected molecular ion (M^+ = 305.2 amu) and fragments associated with successive loss of *tert*-butyl substituents; no higher mass species were detected. Thus, it is suggested that the mutually coupled doublets may be attributed to the presence of the P–H tautomer of **I-*t*Bu**, which is in equilibrium with the N–H tautomer in solution [Eq. (3)].

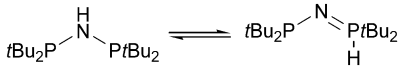

(3)

Support for this proposal comes from the ^1H NMR spectrum of **I-*t*Bu** in C_6D_6, which exhibits a pseudo-triplet (J_{P-H} = 6 Hz) centred at δ 1.17, as a result of virtual coupling, and a broad resonance at δ 1.66 for the N–H tautomer. In addition to these major resonances, the

presence of the P–H tautomer is evident from the observation of two multiplets at δ 1.12 and 1.35 corresponding to the different environments of the two pairs of *tert*-butyl substituents and a doublet at δ 6.03 for the P–*H* proton ($^{1}J_{P-H}$ = 402 Hz), c.f. a doublet at δ 6.03 for the P–*H* proton with $^{1}J_{P-H}$ = 443 Hz in *i*Pr$_2$P(H)NP*i*Pr$_2$(Te).[12]

Although P–H tautomers are formed preferentially for the monochalcogenides *i*Pr$_2$P(H)NP*i*Pr$_2$(E) (E = Se, Te),[12] this intriguing behaviour represents the first reported instance of prototropism for a μ-imidodiphosphine R$_2$PN(H)PR$_2$ (**I**). Detailed variable temperature NMR studies of this process will be the subject of a separate investigation.

The new reagent **I-*t*Bu** is readily metallated by *n*-butylsodium at low temperature (-78 °C) in THF to give the sodium salt NaN(P*t*Bu$_2$)$_2$ (**II-*t*Bu**) as a THF-soluble white powder. The ^{31}P NMR spectrum of **II-*t*Bu** in [D$_8$]THF shows one singlet at δ 101.8. The ^{1}H NMR spectrum of **II-*t*Bu** exhibits a virtual triplet pattern similar to that of **I-*t*Bu**, centred at δ 1.06.

The reactions of **II-*t*Bu** with elemental chalcogens (S, Se, or Te) in the presence of TMEDA in toluene proceed cleanly to give the new sodium complexes **3a-c** as microcrystalline powders in yields of 60 - 81 %. Moderate

air and moisture sensitivity are observed for **3a** and **3b**, whereas **3c** is extremely sensitive to oxygen, particularly in solution. These reagents are soluble in many common organic solvents, and recrystallizations of **3a-c** are best accomplished from saturated toluene solutions. The NMR spectra for **3a-c** in [D_8]THF exhibit similar features. A simple doublet is observed for the *tert*-butyl groups in the ^{1}H NMR spectra and the ^{31}P NMR spectra consist of a singlet, with the selenium and tellurium derivatives, **3b** and **3c**, exhibiting satellites ($^1J_{Se,P}$ = 629 Hz, $^1J_{Te,P}$ = 1490 Hz).

Influence of Chalcogens: Sulfur Systems. We commenced this part of the investigation with an attempt to synthesize the disulfide **4a**, i.e. the sulfur analogue of the known ditelluride **4c**. Efforts to generate **4a** via iodine oxidation of **2a** in THF, under conditions similar to those used for the synthesis of **4c**, resulted in the isolation of a yellow oil. The ^{31}P NMR spectrum of this oil at room temperature revealed a mixture of at least three products, one of which was isolated as colourless crystals and identified as HN(SP*i*Pr$_2$)$_2$ by comparison of ^{31}P NMR and unit-cell parameters with literature values.[21] This product was also formed when the same reaction was carried out in benzene, suggesting the *iso*-propyl substituents may be the source of the hydrogen atom in HN(SP*i*Pr$_2$)$_2$. Consequently, we

turned our attention to the oxidation of the *tert*-butyl derivative **3a**.

In contrast to the behaviour of **2a**, the oxidation of **3a** by one-half an equivalent of iodine in THF proceeded in a straightforward manner to produce the *tert*-butyl substituted disulfide **5a** in 68% yield. The low-temperature ^{31}P NMR spectrum of **5a** exhibited two mutually coupled doublets, consistent with previous observations for **4c**.[12] The structure of **5a** was determined by X-ray crystallography (see Figure 1). Selected bond lengths and bond angles are compared to those of **4c** in Table 1.

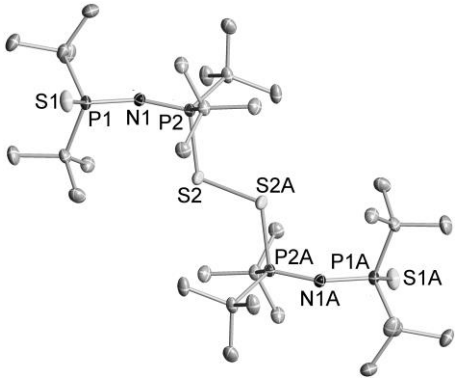

Figure 1. Thermal ellipsoid plot (30 % probability) of the structure of **5a**. The lattice THF molecules and all hydrogen atoms have been omitted for clarity.

Table 1. Selected bond lengths [Å] and bond angles [°] for **4b**, **4c**, **5a** and **5b**.

	4b (E = Se)	**4c** (E = Te)[a]	**5a** (E = S)	**5b** (E = Se)
P(1)-N(1)	1.632(4)	1.623(5)	1.626(2)	1.615(4)
P(2)-N(1)	1.568(4)	1.571(5)	1.554(2)	1.566(4)
P(1)-E(1)	2.135(1)	2.397(2)	1.974(1)	2.135(1)
P(2)-E(2)	2.275(1)	2.489(2)	2.135(1)	2.274(1)
E(1)-E(1a)	2.464(1)	2.946(1)	2.104(2)	2.470(1)
P(1)-N(1)-P(2)	138.0(2)	135.2(3)	151.7(2)	134.7(2)
N(1)-P(1)-E(1)	114.4(1)	114.5(2)	117.9(1)	115.0(2)
N(1)-P(2)-E(2)	108.8(1)	114.1(2)	102.9(1)	112.7(1)
P(1)-E(1)-E(2)	101.17(4)	94.64(5)	109.2(1)	98.09(4)

[a] Data taken from ref. [12].

The metrical parameters of the EPNPE units in **5a** show trends similar to those reported for **4c**.[12] Most notably, there is a substantial difference (ca. 0.14 Å) in the P–S bond lengths; the longer bond involves the sulfur atom that is engaged in the S–S contact. The S–S bond distance in **5a** is 2.104(2) Å, which represents an elongation of only ca. 2% compared to a typical S–S single bond (ca. 2.05 Å).[22] The P–S–S–P torsional angle is 180 °, as was found in the ditelluride dimer **4c**.[12] However, the conformation of the terminal chalcogen atoms of **5a** is quite different from that of **4c**. This is evident in the "S–P–P–S" torsional angle of 109.8 °, which is ca. 80 ° larger than the corresponding angle in **4c**. Another manifestation of this structural difference is reflected in the PNP bond angle of 151.7(2) ° in **5a**, cf. 135.2(3) ° in **4c**. These structural differences may result from a combination of the shorter chalcogen–

chalcogen bond length and the more bulky R groups in **5a** compared to those **4c**.

Influence of Chalcogen: Selenium Systems. In view of the profound influence of a change of R group on the outcome of the iodine oxidation of **2a** and **3a**, our next goal was to determine whether the diselenides **4b** and **5b** are accessible by the one-electron oxidation of **2b** and **3b**, respectively. We found that the reaction of these reagents with one-half equivalent of iodine proceeds cleanly at -78 °C in THF to produce the corresponding dimers **4b** and **5b** as orange powders in ca. 90 % yields.

The room temperature ^{31}P NMR spectra of **4b** and **5b** in [D_8]THF each contain one broad resonance centred at δ 67.3 and 76.3, respectively. At low temperature, this resonance resolves into two mutually coupled doublets, each with ^{77}Se satellites ($^{1}J_{Se,P}$) = 642 and 414 Hz for **4b** and 665 and 439 Hz for **5b**). The low temperature ^{77}Se NMR spectra exhibit two doublets with coupling constants corresponding to those observed in the ^{31}P NMR spectra. The temperature at which the ^{31}P resonances are well resolved is lower for **5b** than for **4b** (193 K vs 213 K). This fluxional behaviour is consistent with the NMR data of the ditelluride **4c**.[12]

Single crystals of **4b** and **5b** suitable for an X-ray structural determination were obtained by recrystallization

of the orange powders from toluene and the molecular structures are depicted in Figures 2 and 3, respectively. Selected bond lengths and bond angles of **4b** and **5b** are compared to those of **4c** and **5a** in Table 1.

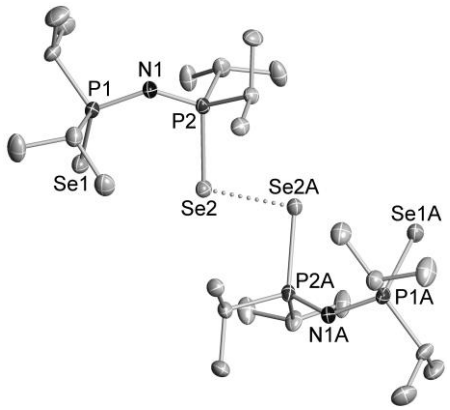

Figure 2. Thermal ellipsoid plot (30 % probability) of the structure of **4b**. The lattice toluene molecule and all hydrogen atoms have been omitted for clarity.

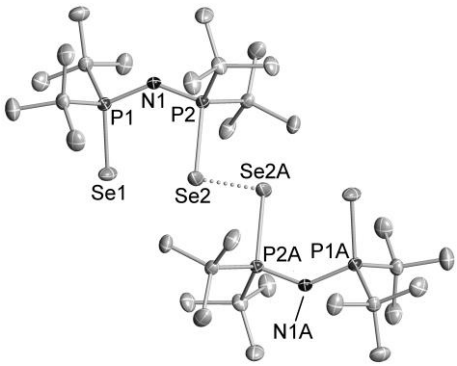

Figure 3. Thermal ellipsoid plot (30 % probability) of the structure of **5b**. All hydrogen atoms have been omitted for clarity.

The metrical parameters of the EPNPE units of the diselenides **4b** and **5b** show very similar trends to those of ditelluride **4c**[12] and the disulfide **5a**. In all these derivatives the P–N bond lengths differ by 0.05-0.06 Å. As

found for **4c** and **5a** (vide supra), there is a substantial difference of ca. 0.14 Å in the phosphorus–selenium bond lengths in both **4b** and **5b**. The selenium–selenium bond lengths (**4b**, 2.470(1) Å; **5b**, 2.464(1) Å) are essentially identical, but elongated by ca. 6 % compared to a typical Se–Se single bond (*c.f.* mean distance of 2.335 Å for diaryl diselenides).[23] The major difference in the structures of **4b** and **5b** involves the P–Se–Se–P torsion angle (155 ° in **4b** vs 180 ° in **5b**, *c.f.* 180 ° in the disulfide **5a** and the ditelluride **4c**). It is possible that a combination of the presence of toluene in the crystal lattice of **4b** together with the different crystal packing forces occasioned by the larger *tert*-butyl groups in **5b** contribute to this disparity. The torsional angles between the two unique selenium atoms (the "Se–P–P–Se" angle) for **4b** and **5b** are 31.5 ° and 33.8 °, respectively, cf. 109.8 ° in **5a**. Significantly, the PNP bond angle in **5b** is 138.0(2) °, *cf.* 151.7(2) ° for **5a**, consistent with the suggestion that the wider bond angle in the sulfur congener **5a** is caused by the short chalcogen–chalcogen bond.

Synthesis and Structure of (TeP*t*Bu$_2$NP*t*Bu$_2$Te–)$_2$ (5c). In addition to completing this systematic study of the one-electron oxidation of the reagents **2a-c** and **3a-c**, the prediction, based on DFT calculations, that the *tert*-butyl

substituted ditelluride (TeP*t*Bu$_2$NP*t*Bu$_2$Te–)$_2$ (**5c**) will have an even longer Te–Te bond length than that in **4c** provide an added incentive for an investigation of the stoichiometric oxidation of **3c** with iodine. This reaction was carried out in the manner described previously for the synthesis of the ditelluride **4c**.[12] The product **5c** was isolated as a dark red powder in 47% yield.

Variable-temperature NMR experiments indicated that the structure of **5c** is fundamentally different from that of the *iso*-propyl analogue **4c**. The ^{31}P NMR spectrum at 298 K showed one broad resonance, which is reminiscent of the fluxional behaviour observed for **4c**.[12] However, upon cooling to 193 K, this resonance was resolved into four broad resonances, indicating the inequivalence of all four phosphorus centres in **5c** in solution at this temperature. By contrast, the ^{31}P NMR spectrum of the *iso*-propyl derivative **4c** at low temperature consists of a pair of mutually coupled doublets, consistent with the solid-state X-ray structure.[12] To account for the disparity between the NMR data of **4c** and **5c**, a crystal structure of **5c** was obtained.

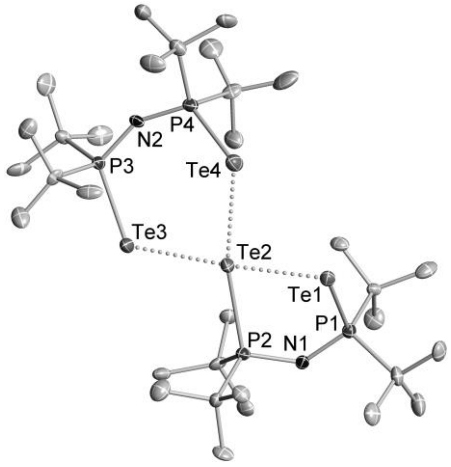

Figure 4. Thermal ellipsoid plot (30 % probability) of the structure of **5c**. All hydrogen atoms have been omitted for clarity

The molecular structure of **5c** is depicted in Figure 4 and selected bond lengths and bond angles are summarized in Table 2. The asymmetric structure of **5c** is consistent with the solution NMR data, and embodies a novel bonding motif for dimers of the type $(EPR_2NPR_2E-)_2$. Instead of existing as a centrosymmetric dimer of two neutral radicals, **5c** can be viewed as the result of an internal redox process in which an electron is transferred from one half to the other half of the dimeric molecule. Thus **5c** may be perceived as a contact ion pair in which the anion $[(TeP\textit{t}Bu_2)_2N]^-$ is *Te,Te'*-chelated to one tellurium atom of the cyclic cation $[(TeP\textit{t}Bu_2)_2N]^+$ (Figure 5).

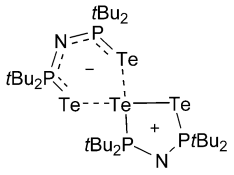

Table 2. Selected bond lengths [Å] and bond angles [°] for **5c**.

	5c
P(1)-N(1)	1.601(8)
P(2)-N(1)	1.619(9)
P(1)-Te(1)	2.451(3)
P(2)-Te(2)	2.637(3)
P(3)-N(2)	1.578(8)
P(4)-N(2)	1.606(9)
P(3)-Te(3)	2.465(3)
P(4)-Te(4)	2.412(3)
Te(1)-Te(2)	2.981(1)
Te(2)-Te(3)	3.102(1)
Te(2)-Te(4)	3.253(1)
P(1)-N(1)-P(2)	132.2(5)
N(1)-P(1)-Te(1)	111.2(3)
N(1)-P(2)-Te(2)	108.9(3)
P(3)-N(2)-P(4)	150.5(6)
N(2)-P(3)-Te(3)	121.1(3)
N(2)-P(4)-Te(4)	117.9(3)

The Te1–Te2–Te3 unit in **5c** forms a nearly linear chain (175.46(3) °). The Te-Te distances of 2.981(1) and 3.102(1) Å in this unit are reminiscent of those in the almost linear anion $[Te_3Ph_3]^-$ (Te-Te 2.939(1) and 3.112(1) Å)[24] and the bent cation $[Te_3Mes_5]^+$ (2.979(1) and 3.049(1) Å),[25] whose structures have been compared to that of the triiodide ion I_3^-. Indeed, we have described the structure of the iodide salt of the cyclic cation $[(TeP\textit{i}Pr_2)_2N]^+$ in a similar manner, since the donation of electron density from

the iodide counter-ion into the LUMO [σ^* (Te–Te)] of the cation results in an elongated Te–Te bond of 2.840(1) Å.[26] In support of this bonding description, the ion-separated salt [(TeP*i*Pr$_2$)$_2$N][SbF$_6$] exhibits a normal Te-Te bond length of 2.7162(7) Å while the chloride salt [(TeP*i*Pr$_2$)$_2$N]Cl displays an elongated Te–Te bond (2.9026(7) Å) indicating a stronger anion–cation interaction than that in [(TeP*i*Pr$_2$)$_2$N]I.[20]

The Te–Te and P–Te bond distances for the cyclic cations in known salts of the type [(TePR$_2$)$_2$N]X are compared with those of **5c** in Table 3. In this context, the description of **5c** as a contact ion pair seems reasonable.[27] The Te1–Te2 bond length of 2.981(1) Å in **5c** implies a significantly stronger interaction of the [(TeP*t*Bu$_2$)$_2$N]$^-$ counter-ion with the cyclic cation than that observed in the related *tert*-butyl substituted iodide salt **7c** (vide infra). The disparity of ca. 0.19 Å in the P–Te bond lengths of the cationic portion of **5c**, *cf*. 0.010 Å in **7c**, is also a reflection of the strong anion–cation interaction. By contrast, the P–Te bond lengths in the anionic part of **5c** differ by only 0.05 Å. The distorted square-planar geometry around Te2 (Σ<(Te2) = 360.13 °) is completed by the Te2–Te4 contact (3.253(1) Å) and the phosphorus atom P2.

Table 3. Structural parameters for $[(TePR_2)_2N]X$

R	X	d(P–Te) (Å)	d(Te–Te) (Å)	Ref.
*i*Pr	SbF_6	2.485(2), 2.497(2)	2.716(1)	[20]
*i*Pr	I	2.396(3), 2.437(3)	2.840(1)	[26]
Ph	I	2.457(1), 2.510(1)	2.846(1)	[20]
*t*Bu	I	2.451(2), 2.550(2)	2.884(1)	[a]
*i*Pr	Cl	2.443(1), 2.500(1)	2.903(1)	[20]
*t*Bu	$(EPtBu_2)_2N$	2.451(3), 2.637(3)	2.981(1)	[a]

[a] This work

DFT Calculations. Three different conformational isomers are observed experimentally for the dichalcogenides in the solid state. The diselenide **4b** adopts a C_2-symmetric conformation whereas the dichalcogenides **4c**, **5a** and **5b** each have molecular structures possessing an inversion centre and, thus, belong to the C_i point group. Even though the latter three structures have the same symmetry group, the conformer observed for **4c** and **5b** differs from that determined for **5a** by the orientation of the terminal chalcogen atoms. Hence, the energy hypersurfaces of systems **4** and **5** were analyzed computationally by performing geometry optimizations for all structures in the three experimentally observed conformations.

The results from geometry optimizations conducted for **4** and **5** are in very good agreement with the existing experimental data (see Supporting Information). The difference in energies of the three conformational isomers for most cases is found to be less than 15 kJ mol^{-1}. For

compounds **4a-c**, the lowest energy isomer adopts a C_2-symmetric structure similar to that observed experimentally for **4b**. However, it must be pointed out that the C_i-symmetric conformer, analogous to the structure observed experimentally for **4c**, is in each case < 5 kJ mol^{-1} higher in energy. Thus, the two conformational isomers are approximately energetically degenerate and the structure adopted in a particular case can easily be influenced by adventitious solvent molecules present in the crystal lattice, as well as slight differences in crystal packing forces. The C_2 symmetric conformer is also found to be the energy minimum for **5b** and **5c**, but not for **5a**, for which the experimentally detected C_i-symmetric structure with twisted terminal chalcogen atoms is ca. 10 kJ mol^{-1} lower in energy.

The structural dichotomy that has been established for the dimers **4c** and **5c** has been probed by DFT calculations of the relative energies of the two isomers **A** and **B** as a function of both the chalcogen and the R group. The results are summarized in Table 4; the relative energies are calculated with respect to the lowest energy conformer found for the dichalcogenide structure **A**.

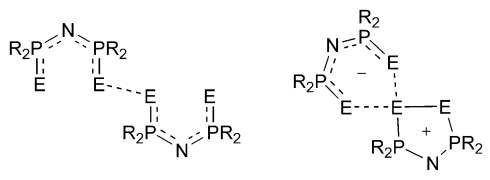

A **B**

Table 4. Relative stabilities of isomers **A** and **B**

	ΔE(**B** – **A**) (kJ mol^{-1})	
	R = *t*Bu	R = *i*Pr
E = S	+15	+25
E = Se	0	+15
E = Te	-20	-2

Although structures analogous to the contact ion pair isomer of **5c** were found for all chalcogen and R-group combinations, a more detailed analysis of the results suggests that the optimized geometries for isomers **B** of the sulfur compounds **4a** and **5a** can be regarded as twisted dichalcogenides rather than true anion–cation structures; in both cases, the E–E–E unit deviates significantly from linearity and displays one short S–S bond (approx. 2.2 Å) and one much longer S···S interaction (3.2 Å for R = *i*Pr and 3.5 Å for R = *t*Bu); the third chalcogen–chalcogen linkage is considerably elongated in both **4a** and **5a**, and exceeds the sum of van der Waals radii for two sulfur atoms in the latter case (see Supporting Information). Thus, the numbers listed for sulfur systems in Table 4 somewhat underestimate the difference in energy between dichalcogenide and contact ion pair structures, as the latter are not stable minima in the energy hypersurface. In comparison, the structural features of the experimentally unknown isomers **B** of selenium and tellurium compounds display geometrical parameters representative of a contact ion pair structure;

the optimized structure of **5c** is also in good agreement with the experimental parameters listed in Table 2.

The energies given in Table 4 show a consistent trend as a function of chalcogen for both the *iso*-propyl and *tert*-butyl series. In both cases, the stability of the contact ion pair structure **B** increases relative to that of the dichalcogenide structure **A** as one descends the series of chalcogens from sulfur to tellurium. However, structure **B** is predicted to be significantly more stable than **A** in only one case (E = Te, R = *t*Bu). While the calculated energies are consistent with the experimental observation of structure **B** for **5c** and structure **A** for the other dimers **4b**, **4c**, **5a** and **5b**, we note that the dichalcogenide structure **A** is not significantly more stable than **B** for the derivatives **4c** and **5b**; the energy difference is practically negligible for both systems. Thus, the calculations raise the intriguing question of whether the contact ion pair structure might be kinetically stabilized in those cases by using an alternative synthetic approach, viz. direct reactions between an acyclic anion $[EPR_2NPR_2E]^-$ and the corresponding cyclic cation $[(EPR_2)_2N]^+$ (E = Se, Te; R = *i*Pr, *t*Bu) This approach could also be used to investigate the feasibility of generating mixed chalcogen dimers.

Synthesis and Structures of [(EP*t*Bu$_2$)$_2$N]X (7a, E = S, X = I$_3$; 7b, E = Se, X = I; 7c, E = Te, X = I). The preceding findings on the one-electron oxidation of the *tert*-butyl substituted reagents **3a-c,** together with our recent report of the two-electron oxidation of the *iso*-propyl-substituted derivatives **2b** or **2c** to give iodide salts of the cyclic cations [(EP*i*Pr$_2$)$_2$N]$^+$ (E = Se, Te) [Eq. (4)],[20,26] raise a number of questions related to the two-electron oxidation of the new reagents **3a**–**3c,** which are addressed in this final section.

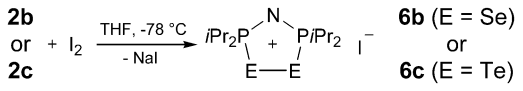

(4)

The *iso*-propyl-substituted sulfur-containing cation [(SP*i*Pr$_2$)$_2$N]$^+$ was not obtained as the iodide salt **6a** by the route depicted in [Eq. (4)].[20] In the context of the complications observed in the one-electron oxidation of **2a** in this work, the lack of success is understandable. Concomitantly, the efficient synthesis of the *tert*-butyl-substituted disulfide **5a** by one-electron oxidation of **3a** begs the question of whether the corresponding cation [(SP*t*Bu$_2$)$_2$N]$^+$ can be obtained by the stoichiometric oxidation of **3a** with iodine. The reaction of **3a** with one equivalent of iodine resulted in the isolation of a poorly soluble dark yellow solid. The recrystallization of this

solid from hot toluene yielded several dark orange single crystals which were identified by an X-ray structural determination as $[(SPtBu_2)_2N]I_3$ (**7a**). Compound **7a** can be obtained in 73 % yield by carrying out the reaction of **3a** with iodine in a 1:2 molar ratio.

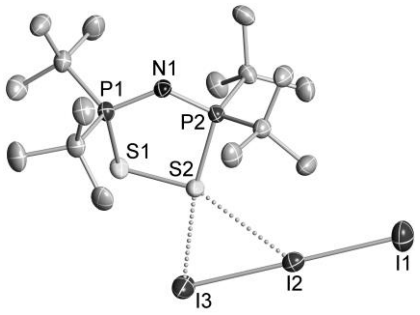

Figure 6. The structure of **7a**. Hydrogen atoms have been omitted for clarity.

As illustrated in Figure 6, compound **7a** is an ion-separated salt comprised of the five-membered cyclic cation $[(SPtBu_2)_2N]^+$ and a triiodide counterion. This is the first example of the S_2P_2N ring system.[28] Selected bond lengths and bond angles of **7a** are given in Table 5. The closest S–I distances observed are S2–I3 (3.620(1) Å) and S2–I2 (3.726(1) Å).[29] The S–S bond distance in the cation is 2.084(2) Å, close to the single-bond value and is slightly less than the value of 2.104(2) Å observed in the acyclic disulfide **5a**. [22] Both pairs of P–N and P–S bond distances are essentially equal in the cationic five-membered ring of **7a**. The mean P–S bond distance of 2.125 Å can be compared

with the values of 1.974 and 2.135 Å in the acyclic dimer **5a**.

Table 5. Selected bond lengths [Å] and bond angles [°] for **7a-c**.

	7a (E = S)	**7b** (E = Se)	**7c** (E = Te)
P(1)-N(1)	1.594(3)	1.605(3)	1.596(4)
P(2)-N(1)	1.597(3)	1.604(3)	1.600(4)
P(1)-E(1)	2.131(2)	2.307(2)	2.550(2)
P(2)-E(2)	2.120(2)	2.220(1)	2.451(2)
E(1)-E(2)	2.084(2)	2.502(1)	2.884(1)
I(1)-I(2)	2.913(1)		
I(2)-I(3)	2.931(1)		
E(1)-I(1)		3.061(1)	3.162(1)
E(1)-E(2)'		3.466(2)	3.585(2)
P(1)-N(1)-P(2)	124.1(2)	128.7(2)	134.4(3)
N(1)-P(1)-E(1)	105.0(1)	107.2(1)	108.6(2)
N(1)-P(2)-E(2)	105.0(1)	107.6(1)	109.0(2)
P(1)-E(1)-E(2)	96.5(1)	91.1(1)	87.1(1)
P(2)-E(2)-E(1)	96.9(1)	93.1(1)	89.2(1)
I(1)-I(2)-I(3)	178.8(1)		
P(1)-E(1)-I(1)		104.4(1)	102.6(1)
I(1)-E(1)-E(2)		164.3(1)	170.1(1)

The presence of an incipient cation $[(TeP\textit{t}Bu_2)_2N]^+$ in the dimer **5c**, prompted an investigation of the synthesis of this cation by the two-electron oxidation of **3c** with iodine. This reaction produced a dark crystalline material in 78 % yield. The selenium analogue **7b** was prepared in the same manner from **3b** and isolated in 88 % yield as a dark orange solid. The structures of both **7b** and **7c** were determined by X-ray crystallography to be $[(EP\textit{t}Bu_2)_2N]I$ (E = Se, Te) (Figure 7). Selected bond lengths and bond angles for **7b** and **7c** are displayed in Table 5.

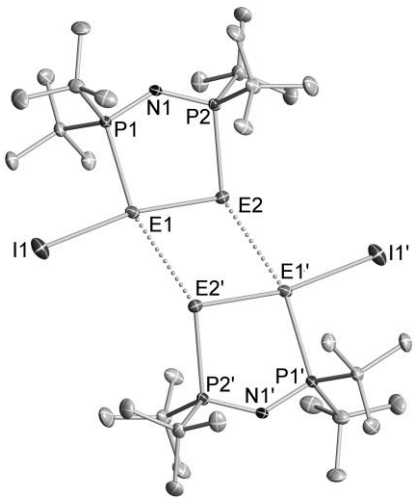

Figure 7. The structure of **7b** (E = Se) and **7c** (E = Te). Hydrogen atoms have been omitted for clarity.

In contrast to the linear chains formed in **6b** and **6c,**[26] the *tert*-butyl derivatives **7b** and **7c** both exhibit a dimeric structure in which two five-membered $[(EP\mathit{t}Bu_2)_2N]^+$ (E = Se, Te) cations are associated by E···E contacts and one chalcogen atom of each cation is linked to an iodine atom. Interestingly, the chalcogen distance within the cationic rings is significantly longer (by 0.018 Å and 0.044 Å for **7b** and **7c,** respectively) than the value reported for the *iso*-propyl analogues **6b** and **6c.**[26] The intermolecular E···E distances of 3.466(2) and 3.585(2) Å in **7b** and **7c,** respectively, correspond to a significant van der Waals interaction.[29] The E–I distances in **7b** and **7c** are substantially shorter by 0.089 Å and 0.268 Å, respectively, than the values observed in the corresponding *iso*-propyl derivatives **6b** and **6c.**[26] This disparity is presumably

related to the fundamental difference in these two structures. The iodide ion is coordinated to only one tellurium atom in **7b** and **7c**, whereas it performs a bridging function in **6b** and **6c**. DFT calculations have shown that the elongation of the chalcogen–chalcogen bond lengths in the cations of **6b** and **6c** is the result of donation of electron density from iodide ion to the σ* orbital (LUMO) of the cation.[26] Thus, the elongation of the E–E bond in **7b** and **7c** can be attributed to the stronger E–I interaction in those salts. Finally, we draw attention to the structural similarities between the cation in **7c** and the cationic part of the tellurium-centred dimer **5c** (Table 3) in support of the description of **5c** as a cation–anion pair.

Conclusions

A systematic investigation of the one-electron oxidation of dichalcogenoimidodiphosphinate anions $[(EPR_2)_2N]^-$ (E = S, Se, Te; R = *i*Pr, *t*Bu) with iodine has shown that, with one exception (E = S, R = *i*Pr) the formation of dichalcogenide dimers is a common feature for all three chalcogens. For the tellurium-containing systems these studies also revealed the existence of two structural isomers, a dichalcogenide and a spirocyclic contact ion

pair. The two-electron oxidation of the new *tert*-butyl derivatives $[EPtBu_2NPtBu_2E]^-$ [E = S, Se, Te] produced the cyclic cations $[(EPtBu_2)_2N]^+$, including the first example of the five-membered S_2P_2N ring system, as iodide or triiodide salts. Consideration of the trends in the calculated relative energies of the two structural isomers for the dimers $(EPR_2NPR_2E-)_2$ raises the possibility of preparing other spirocyclic contact ion pairs or mixed chalcogen dimeric systems by the reactions of an acyclic anion $[(EPR_2)_2N]^-$ with a cyclic cation $[(E'PR_2)_2N]^+$ ($E \neq E'$). An evaluation of the feasibility of this approach will be the subject of future investigations.

Experimental Section

Reagents and General Procedures. THF, toluene, hexane and benzene were dried and distilled over Na/benzophenone; dichloromethane was dried and distilled over calcium hydride. All solvents were stored over 4 Å molecular sieves prior to use. Grey selenium and tellurium powders were washed with methanol and dried under vacuum. Sodium amide (Acros Organics), sodium hydride (Aldrich), *N,N,N′,N′*-tetramethylethylenediamine (Aldrich), iodine (Aldrich) and di-*tert*-butylchlorophosphine (Aldrich) were used as received. n-Butylsodium,[30] $HN(PiPr_2)_2$ (**I-*i*Pr**)[21] and

$NaN(PiPr_2)_2$ (**II-*i*Pr**)[6] were prepared according to modifications of the literature procedures. All manipulations were performed under an inert atmosphere of argon using standard Schlenk techniques.

Instrumentation. ^{1}H, ^{31}P, and ^{77}Se NMR were recorded on either a Bruker AC-300 or AMX-300 NMR spectrometer, with chemical shifts reported relative to Me_4Si (^{1}H), 85 % H_3PO_4 (^{31}P), Se_2Ph_2 (^{77}Se) and Te_2Ph_2 (^{125}Te). Chemical shifts are reported in parts per million (ppm). Elemental analyses were performed by the Analytical Services Laboratory, Department of Chemistry, University of Calgary, and Canadian Microanalytical Service Ltd (Delta, British Columbia).

Computational Details. DFT calculations were performed for various geometrical and conformational isomers of compounds **4** and **5** (see text for details). The molecular structures were optimized by using a combination of the hybrid PBE0 exchange-correlation functional[31] with the Ahlrichs' triple-zeta valence basis set augmented by one set of polarization functions (TZVP);[32] for tellurium, the corresponding ECP basis set was used. All calculations were performed with the Turbomole 5.8[33] program package.

Synthesis of 2a. A cold (0 °C) suspension of S_8 (0.142 g, 0.554 mmol) in toluene (25 mL) was added to a solution

of **II-*i*Pr** (0.601 g, 2.22 mmol) in toluene (25 mL) containing TMEDA (0.33 mL, 2.2 mmol) at 0 °C, producing a pale yellow mixture. After heating to 50 °C for 1 h, the solution was filtered through a 0.45 μm pore size filter disk and the solvent was removed in vacuo to yield a yellow oil, which solidified on standing to give **2a** as an off-white powder (0.836 g, 84 %). NMR Data ([D$_8$]THF): ^{1}H: δ = 2.30 (s, 4H, -N(C*H*$_2$)$_2$N-), 2.16 (s, 12 H, (C*H*$_3$)$_2$N-), 1.82 (m, 4H, -C*H*(CH$_3$)$_2$), 1.12 (m, 24H, -CH(C*H*$_3$)$_2$); ^{31}P: δ = 63.3 (s); elemental analysis calcd (%) (for loss of half an equivalent of TMEDA) for $C_{15}H_{36}N_2NaP_2S_2$ (393.53): C 45.78, H 9.22, N 7.12; found: C 45.27, H 8.85, N 7.23.

Synthesis of 2b. A suspension of the reagent **II-*i*Pr** (0.999 g, 3.68 mmol) and grey selenium powder (0.583 g, 7.38 mmol) in toluene (25 mL) containing TMEDA (0.56 mL, 3.7 mmol) was heated to 80 °C and stirred for 2 h. Filtration through a 0.45 μm pore size filter disk afforded a pale yellow solution and, after removal of the solvent in vacuo, a yellow oil remained. The oil was dissolved in hexane and solvent was removed under vacuum (2 x 10 mL) to give **2b** as a pale yellow solid (1.654 g, 82 %). NMR Data ([D$_8$]THF): ^{1}H: δ = 2.30 (s, 4H, -N(C*H*$_2$)$_2$N-), 2.16 (s, 24H, (C*H*$_3$)$_2$N-), 1.85 (m, 4H, -C*H*(CH$_3$)$_2$), 1.13 (m, 24H, -CH(C*H*$_3$)$_2$);

^{31}P: δ = 53.5 (s, $^{1}J_{Se,P}$ = 618 Hz); ^{77}Se: δ = -315 ($^{1}J_{Se,P}$ = 620 Hz); elemental analysis calcd (%) for $C_{18}H_{44}N_3NaP_2Se_2$ (545.4): C 39.64, H 8.13, N 7.70; found: C 39.69, H 8.16, N 7.58.

Synthesis of I-*t*Bu. A clear colourless solution of di-*tert*-butylchlorophosphine (3.550 g, 19.65 mmol) in THF (25 mL) was added to a white suspension of sodium amide (0.769 g, 19.7 mmol) in THF (25 mL) by using a cannula. The resulting white suspension was stirred at 60 °C for 2 h. The solvent was then removed from the resulting cloudy white suspension in vacuo, affording a gummy white solid. To this was added hexane (30 mL), to give a white suspension which was filtered through celite over a 0.45 μm pore size filter disk and collected in a new flask. Removal of solvent from the resulting clear colourless solution yielded a white crystalline solid which was dried under vacuum to yield **I-*t*Bu** (1.564 g, 52 %). NMR data ([D_6]benzene): ^{1}H: δ = 1.66 (br s, 1H, N-*H*), 1.17 (virtual t, 36H, $J_{P,H}$ = 6 Hz, -C(C*H*$_3$)$_3$); ^{31}P: δ = 83.0 (s, N-H tautomer), [87.5 (d, $^{2}J_{P,P}$ = 43 Hz), 40.0 (d, $^{2}J_{P,P}$ = 43 Hz), P-H tautomer]; MS (EI): 305.2 (M^+); elemental analysis calcd (%) for $C_{16}H_{37}NP_2$ (305.4): C 62.92, H 12.21, N 4.59; found: C 62.74, H 12.66, N 4.58.

Synthesis of II-*t*Bu. A cold (-78°C) solution of *n*BuNa (0.530 g, 6.62 mmol) in a mixture of hexane (5 mL) and THF (15 mL) was added slowly (by cannula) to a solution of **I-*t*Bu** (2.000 g, 6.548 mmol) in THF (40 mL) at -78 °C. The resulting clear colourless solution was stirred at -78 °C for 2 h and then allowed to warm to room temperature. The solvents were removed in vacuo, and the solid residue was washed with hexane (2 x 10 mL) and dried in vacuo to yield **II-*t*Bu** as a white powder (1.115 g, 52 %). NMR data ([D_8]THF): ^{1}H (298 K): δ = 1.06 (virtual t, $J_{P,H}$ = 6 Hz); ^{31}P: δ = 101.8 (s); elemental analysis calcd (%) for $C_{16}H_{36}NNaP_2$ (327.4): C 58.70, H 11.08, N 4.28; found: C 57.56, H 10.89, N 4.64.

Synthesis of 3a. A cold (0 °C) solution of S_8 (0.054 mg, 0.21 mmol) in toluene (20 mL) was added by cannula to a suspension of **II-*t*Bu** (0.275 g, 0.84 mmol) in toluene (20 mL) containing TMEDA (0.14 mL, 0.93 mmol) at 0 °C. The resulting cloudy yellow solution was stirred at 0 °C for 10 min, then warmed to room temperature and heated to 50 °C for 1 h. The resulting suspension was filtered through a 0.45 μm pore size filter disk to afford a clear yellow solution. The solvent was removed in vacuo to give a crude yellow powder, which was recrystallized from hexane to give

3a as a pale yellow crystalline solid (0.255 g, 60 %). NMR data ([D_8]THF): ^{1}H δ = 2.31 (s, 4H, -N(C*H*$_2$)$_2$N-), 2.15 (s, 12H, (C*H*$_3$)$_2$N-), 1.35 (d, $^{3}J_{P,H}$ = 15 Hz, -C(C*H*$_3$)$_3$); ^{31}P δ = 69.9 (s); elemental analysis calcd (%) for $C_{22}H_{52}N_3NaP_2S_2$ (507.7): C 52.04, H 10.32, N 8.28; found: C 52.09, H 10.53, N 8.16.

Synthesis of 3b. A suspension of **II-*t*Bu** (0.350 g, 1.07 mmol) and grey selenium powder (0.170 g, 2.15 mmol) in toluene (25 mL) containing TMEDA (0.18 mL, 1.2 mmol) was heated to 80 °C, stirred for 2 h and then filtered through a 0.45 μm pore size filter disk to afford a clear orange solution. The solvent was then removed in vacuo to give a crude orange powder, which was recrystallized from hexane to give **3b** as a colourless crystalline solid (0.594 g, 77 %). NMR data ([D_8]THF): ^{1}H: δ = 2.30 (s, 4H, (CH$_3$)$_2$N(C*H*$_2$)$_2$N(CH$_3$)$_2$), 2.15 (s, (C*H*$_3$)$_2$N(CH$_2$)$_2$N(C*H*$_3$)$_2$), 1.37 (d, $^{3}J_{P,H}$ = 15.3 Hz, 36H, P((C*H*$_3$)$_3$)$_2$); ^{31}P: δ = 65.9 (s, $^{1}J_{Se,P}$ = 629 Hz); ^{77}Se: δ = -298 (d, $^{1}J_{Se,P}$ = 627 Hz); elemental analysis calcd (%) for $C_{22}H_{52}N_3NaP_2Se_2$ (601.5): C 43.93, H 8.71, N 6.99; found: C 43.60, H 8.52, N 6.78.

Synthesis of 3c. The synthesis of **3c** was carried out in a manner similar to that of **3b**. **II-*t*Bu** (0.469 g, 1.43 mmol), tellurium (0.375 g, 2.94 mmol) and TMEDA (0.25 mL, 1.7 mmol) reacted to produce an oil, which was washed with

hexane (2 x 10 mL) and dried in vacuo to give **3c** as a yellow micro-crystalline solid (0.807 g, 81 %). NMR Data ([D$_8$]THF): ^{1}H: δ = 2.30 (s, 4H, (CH$_3$)$_2$N(C*H*$_2$)$_2$N(CH$_3$)$_2$), 2.15 (s, 12H, (C*H*$_3$)$_2$N(CH$_2$)$_2$N(C*H*$_3$)$_2$), 1.37 (d, $^3J_{P,H}$ = 16 Hz, 36H, -C(C*H*$_3$)$_3$); ^{31}P: δ = 41.2 (s, $^1J_{Te,P}$ = 1490 Hz); ^{125}Te: δ = -713 ($^1J_{Te,P}$ = 1487 Hz); elemental analysis calcd (%) for $C_{22}H_{52}N_3NaP_2Te_2$ (698.8): C 37.81, H 7.50, N 6.01; found: C 38.13, H 8.23, N 5.80.

Synthesis of 4b. A cold (-78 °C) solution of I_2 (0.019 g, 0.075 mmol) in THF (25 mL) was added by cannula to a solution of **2b** (0.082 g, 0.15 mmol) in THF (25 mL) at -78 °C. The mixtured was stirred at -78 °C for 30 min and then at room temperature for an additional 30 min. The solvent was removed in vacuo and the residue was dissolved in hexane to produce a suspension, which was filtered through a 0.45 µm pore size filter disk. Removal of hexane from the filtrate in vacuo produced **4b** as a dark orange powder (0.055 g, 90 %). NMR data ([D$_8$]THF): ^{1}H (298 K): δ = 2.36 (broad s, 8H), 1.28 (broad m, 48H); ^{31}P (298 K): δ = 67.3 (broad s); (213 K): δ = 69.4 (d, $^2J_{P,P}$ = 29 Hz, $^1J_{Se,P}$ = 642 Hz), 65.2 (d, $^2J_{P,P}$ = 29 Hz, $^1J_{Se,P}$ = 414 Hz); ^{77}Se (298 K): no detectable resonance; (213 K): δ = 241.9 (d, $^1J_{Se,P}$ = 411 Hz), -145 (broad d, $^1J_{Se,P}$ = 640 Hz); elemental analysis

calcd (%) for $C_{24}H_{56}N_2P_4Se_4$ (812.5): C 35.48, H 6.95, N 3.45; found: C 35.36, H 7.00, N 3.26. X-ray quality crystals of **4b**•C_7H_8 were obtained from a warm saturated toluene solution upon cooling to room temperature.

Synthesis of 5a. The synthesis of **5a** was carried out in a similar manner to that of **4b**. A mixture of **3a** (0.100 g, 0.197 mmol) and I_2 (0.026 g, 0.10 mmol) produced a pale yellow powder (0.050 g, 68 %). NMR Data ([D_8]THF): ^{1}H (298 K) δ = 1.50 (broad d, $^3J_{31P-1H}$ = 16 Hz); ^{31}P (298 K) δ = 79.4 (broad s), 63.1 (broad s); (233 K) δ = 78.9 (d, $^3J_{P,P}$ = 51 Hz), 62.2 (d, $^3J_{P,P}$ = 51 Hz); elemental analysis calcd (%) for $C_{32}H_{72}N_2P_4S_4$ (737.1): C 52.14, H 9.85, N 3.80; found: C 51.82, H 9.61, N 3.63. X-ray quality crystals of **5a**•2(C_4H_8O) were obtained from a concentrated THF solution upon cooling to -18 °C

Synthesis of 5b. The synthesis of **5b** was carried out in a similar manner to that of **4b**. The reaction of **3b** (0.200 g, 0.332 mmol) and I_2 (0.041 g, 0.16 mmol) produced **5b** as an orange powder (0.133 g, 89 %). NMR data ([D_8]THF): ^{1}H (298 K): δ = 1.51 (m); ^{31}P (298 K): δ = 76.3 (broad s, $^1J_{Se,P}$ = ca. 540 Hz; (193 K): 78.1 (d, $^3J_{P,P}$ = 44 Hz, $^1J_{Se,P}$ = 665 Hz), 68.6 (d, $^3J_{P,P}$ = 44 Hz, $^1J_{Se,P}$ = 439 Hz); ^{77}Se (298 K): no detectable resonance; (193 K): δ = 304 (d, $^1J_{Se,P}$ =

439 Hz), -128 (d, $^{1}J_{Se,P}$ = 670 Hz); elemental analysis calcd (%) for $C_{32}H_{72}N_2P_4Se_4$ (924.7): C 41.57, H 7.85, N 3.03; found: C 41.95, H 7.76, N 3.01. X-ray quality crystals of **4b** were obtained from a warm saturated toluene solution upon cooling to room temperature.

Synthesis of 5c. The synthesis of **5b** was carried out in a similar manner to that of **4b**. The reaction of **3c** (0.200 g, 0.286 mmol) and I_2 (0.036 g, 0.14 mmol) produced **5c** as a dark red powder (0.075 mg, 47 %). NMR data ([D_8]THF): ^{1}H (298 K): δ = 1.49 (d, $^{3}J_{P,H}$ = 16 Hz); ^{31}P (298 K): δ = 58.8 (v. broad s); (193 K): δ = 71.3 (br, s), 59.5 (br, s), 54.4 (br, s), 46.8 (br, s); elemental analysis calcd (%) for $C_{32}H_{72}N_2P_4Te_4$ (1119.2): C 34.34, H 6.48, N 2.50; found: C 35.72, H 5.90, N 2.44. X-ray quality crystals of **5c** were obtained from slow diffusion of hexane into a concentrated THF solution at -30 °C.

Synthesis of 7a. A cold (-78 °C) solution of I_2 (0.102 mg, 0.402 mmol) in THF (15 mL) was added slowly (by cannula) to a solution of **3a** (0.102 g, 0.201 mmol) in THF (15 mL) at -78 °C. The resulting clear orange solution was stirred at -78 °C for 30 min, then warmed to room temperature and stirred for an additional 30 min. The solvent was then removed in vacuo to afford a brown solid to which dichloromethane (10 mL) was added. The resulting

suspension was filtered through a 0.45 μm pore size filter disk to yield a dark orange solution. Upon slow removal of the solvent in vacuo, dark yellow-brown needles formed. The resulting mixture of crystalline material and brown oil was washed with hexane (10 mL) and the crystals of **7a** were dried under vacuum (0.100 g, 73 %). NMR data (CD_2Cl_2): ^1H: δ = 1.55 (m); ^{31}P: δ = 129.3 (br. s); elemental analysis calcd (%) for $C_{16}H_{36}I_3NP_2S_2$ (749.26): C 25.65, H 4.84, N 1.87; found: C 24.80, H 4.68, N 2.42.

Synthesis of 7b. The synthesis of **7b** was carried out in a similar manner to that of **7a**. The reagent **3b** (0.200 g, 0.332 mmol) and I_2 (0.085 mg, 0.33 mmol) reacted to produce **7b** as a dark orange powder (0.173 g, 88 %). NMR data (CD_2Cl_2): ^1H: δ = 1.56 (d, $^3J_{P,H}$ = 18 Hz); ^{31}P: δ = 117.5 (s, $^1J_{Se,P}$ = 392 Hz); ^{77}Se: δ = 456 (d, $^1J_{Se,P}$ = 393 Hz); elemental analysis calcd (%) for $C_{16}H_{36}INP_2Se_2$ (589.2): C 32.61, H 6.16, N 2.38; found: C 31.86, H 6.07, N 2.66.

Synthesis of 7c. The synthesis of **7c** was carried out in a similar manner to that of **7a**. The reagent **3c** (0.102 g, 0.146 mmol) and I_2 (0.037 g, 0.15 mmol) reacted to produce **7c** as a dark red microcrystalline solid (0.078 g, 78 %). NMR data (CD_2Cl_2): ^1H: δ = 1.55 (d, $^3J_{P,H}$ = 17 Hz); ^{31}P: δ = 83.5 ($^1J_{Te,P}$ = 959 Hz); ^{125}Te: δ = 485 ($^1J_{Te,P}$ = 954 Hz);

elemental analysis calcd (%) for $C_{16}H_{36}INP_2Te_2$ (686.5): C 27.99, H 5.29, N 2.04; found: C 28.59, H 5.22, N 2.08.

X-ray structural determinations. A suitable crystal of the complex was selected, coated in Paratone oil and mounted on a glass fibre. Data were collected at 173 K on a Nonius KappaCCD diffractometer using $Mo_{K\alpha}$ radiation (λ = 0.71073 Å) with ω and ϕ scans. The unit-cell parameters were calculated and refined from the full data set. Crystal cell refinement and data reduction were carried out by using the Nonius DENZO package. After data reduction, the data were corrected for absorption based on equivalent reflections using SCALEPACK (Nonius, 1998). The structures were solved by direct methods using SHELXS-97 and refinement was carried out on F^2 against all independent reflections by the full-matrix least-squares method using the SHELXL-97 program.[34] The hydrogen atoms were calculated geometrically and were riding on their respective atoms, and all non-hydrogen atoms were refined with anisotropic thermal parameters. CCDC-631684 to CCDC-631690 contain the supplementary crystallographic data for this paper. These data can be obtained free of charge from the Cambridge Crystallographic Data Centre via www.ccdc.cam.ac.uk/data_request/cif.

Crystallographic data are summarized in Tables 6 and 7.

Table 6. Crystal data and structure refinements for complexes **4b•C_7H_8**, **5a•2(C_4H_8O)** and **5b**

	4b•C_7H_8	**5a•2(C_4H_8O)**	**5b**
empirical formula	$C_{31}H_{64}N_2P_4Se_4$	$C_{40}H_{88}N_2O_2P_4S_4$	$C_{32}H_{72}N_2P_4Se_4$
formula weight	904.56	881.24	924.64
crystal system	monoclinic	monoclinic	monoclinic
space group	*C*2/*c*	$P2_1/c$	$P2_1/n$
a [Å]	25.162(5)	11.963(2)	8.964(2)
b [Å]	14.300(3)	10.876(2)	12.976(3)
c [Å]	11.636(2)	19.559(4)	18.125(4)
β [°]	92.20(3)	98.58(3)	91.89(3)
V [Å^3]	4183.6(14)	2516.2(8)	2106.9(7)
Z	4	2	2
ρ_{calcd} [g cm^{-3}]	1.436	1.163	1.457
μ ($Mo_{K\alpha}$) [mm^{-1}]	3.683	0.349	3.658
reflections collected	17200	21728	15157
independent reflections	3675	4431	3694
parameters	192	245	202
goodness-of-fit on F^2	1.047	1.043	1.123
final R indices [$I>2\sigma(I)$] R_1, wR_2	0.0398, 0.0914	0.0488, 0.1116	0.0414, 0.0920
R indices (all data) $R1$, wR_2	0.0664, 0.1054	0.0923, 0.1323	0.0673, 0.1023
largest diff. peak/hole [e Å^{-3}]	0.694/-0.504	0.301/-0.453	0.681/-0.466

Table 7. Crystal data and structure refinements for complexes **5c, 7a, 7b** and **7c.**

	5c	**7a**	**7b**	**7c**
empirical formula	$C_{32}H_{72}N_2P_4Te_4$	$C_{16}H_{36}I_3NP_2S_2$	$C_{16}H_{36}INP_2Se_2$	$C_{16}H_{36}INP_2Te_2$
formula weight	1119.20	749.22	589.22	686.50
crystal system	monoclinic	monoclinic	triclinic	triclinic
space group	$P2_1/n$	$P2_1/n$	$P\bar{1}$	$P\bar{1}$
a [Å]	8.888(2)	13.918(3)	8.533(2)	8.548(2)
b [Å]	37.854(8)	10.266(2)	11.204(2)	11.387(2)
c [Å]	13.122(3)	18.700(4)	12.854(3)	13.096(3)
α [°]	90	90	69.70(3)	71.33(3)
β [°]	91.37(3)	101.03(3)	77.88(3)	81.15(3)
γ [°]	90	90	12.854(3)	88.53(3)
V [Å^3]	4413.7(16)	2622.5(10)	1125.1(5)	1192.9(5)
Z	4	4	2	2
ρ_{calcd} [gcm^{-3}]	1.684	1.898	1.739	1.911
μ ($Mo_{K\alpha}$) [mm^{-1}]	2.785	3.859	4.799	3.872
reflections collected	26653	44178	13792	20169
independent reflections	7756	5998	5046	5395
parameters	403	229	212	212
goodness-of-fit on F^2	1.015	1.028	1.110	1.070
final R indices [$I>2\sigma(I)$] R_1, wR_2	0.0607, 0.1132	0.0375, 0.0795	0.0411, 0.1175	0.0424, 0.1151
R indices (all data) $R1$, wR_2	0.1335, 0.1371	0.0693, 0.0913	0.0462, 0.1210	0.0534, 0.1227
largest diff. peak/hole [e Å^{-3}]	1.658 /-1.038	0.969/-1.058	0.879/-0.930	1.374/-1.060

No special considerations were necessary for the refinements of compounds **5b, 5c, 7a, 7b** and **7c.**

Compound ***4b***: The disordered lattice toluene molecule was modeled as a 75:25 isotropic mixture. Refinement of the model for the 25 % portion was further complicated by disorder of the methyl group across a symmetry element. This portion was modelled as a 50:50 mixture of benzene and *o*-xylene. Only one-half of **4b** was located in the difference Fourier map, as the molecule is situated on a crystallographic two-fold axis.

Compound ***5a***: The disordered solvent THF molecule was modeled isotropically as a 50:50 mixture across two positions. One-half of **5a** was located in the difference Fourier map, as the molecule sits on a crystallographic inversion centre.

Acknowledgements

The authors gratefully acknowledge NSERC (Canada) (DJE and JSR), Alberta Ingenuity (DJE and JSR) and the Academy of Finland (HMT) for financial support.

References

[1] a) C. Silvestru, J. E. Drake, *Coord. Chem. Rev.* **2001**, *223*, 117-216; b) J. D. Woollins, *J. Chem. Soc. Dalton Trans.* **1996**, 2893-2901; c) I. Haiduc, in *Comprehensive Coordination Chemistry II*, J. A. McCleverty, T. J. Meyer (Eds.) Elsevier Ltd, Amsterdam, **2003**, pp. 323-347.

[2] See, for example: a) M. Afzall, D. Crouch, M. A. Malik, M. Motevalli, P. O'Brien, J.-H. Park, J. D. Woollins, *Eur. J. Inorg. Chem.* **2004**, 171-177; b) D. J. Crouch, P. M. Hatton, M. Helliwell, P. O'Brien, J. Raftery, *Dalton Trans.* **2003**, 2761-2766.

[3] D. J. Crouch, P. O'Brien, M. A. Malik, P. J. Skabara, S. P. Wright, *Chem. Commun.* **2003**, 1454-1455.

[4] a) R. Cea-Olivares, J. Novosad, J. D. Woollins, A. M. Z. Slawin, V. García-Montalvo, G. Espinosa-Pérez, P. G. y García, *Chem. Commun*. **1996**, 519-520; b) R. Cea-Olivares, G. Canseco-Melchor, V. García-Montalvo, S. Hernández-Ortega, J. Novosad, *Eur. J. Inorg. Chem*. **1998**, 1573-1576; c) R. Cea-Olivares, M. Moya-Cabrera, V. García-Montalvo, R. Castro-Blanco, R. A. Toscano, S. Hernández-Ortega, *Dalton Trans*. **2005**, 1017-1018.

[5] T. Chivers, G. G. Briand, M. Parvez, *Angew. Chem.* **2002**, *114*, 3618-3620; *Angew. Chem. Int. Ed.* **2002**, *41*, 3468-3470.

[6] T. Chivers, D. J. Eisler, J. S. Ritch, *Dalton Trans.* **2005**, 2675-2677.

[7] A. J. Gaunt, B. L. Scott, M. P. Neu, *Angew. Chem.* **2006**, *118*, 1668-1671; *Angew. Chem. Int. Ed*. **2006**, *45*, 1638-1641.

[8] M. C. Copsey and T. Chivers, *Chem. Commun*. **2005**, 4938-4940.

[9] S. S. Garje, J. S. Ritch, D. J. Eisler, M. Afzaal, P. O'Brien, T. Chivers, *J. Mater. Chem.* **2005**, *16,* 966-969.

[10] S. S. Garje, M. C. Copsey, M. Afzaal, P. O'Brien, T. Chivers, *J. Mater. Chem.* **2006**, *16*, 4542-4547.

[11] S. S. Garje, D. J. Eisler, J. S. Ritch, M. Afzaal, P. O'Brien, T. Chivers, *J. Am. Chem. Soc*. **2006**, *128*, 3120-3121.

[12] T. Chivers, D. J. Eisler, J. S. Ritch, H. M. Tuononen, *Angew. Chem.* **2005**, *117*, 5033-5036; *Angew. Chem. Int. Ed.* **2005**, *44*, 4953-4956.

[13] The Te-Te bond lengths of ditellurides are typically in the range 2.68-2.71 Å, but a value of 2.77 Å has been reported recently for the highly crowded system $(PhMe_2Si)_3CTe\text{-}TeC(SiMe_2Ph)_3$. T. M. Klapötke, B. Krumm, H. Nöth, J. C. Gálvez-Ruiz, K. Polborn, I. Schwab, M. Suter, M. *Inorg. Chem.* **2005**, *44*, 5254-5265.

[14] J. E. McDonough, J. J. Weir, M. J. Carlson,C. D. Hoff, O. P. Kryatova, E. V. Rybak-Akimova, C. R. Clough, C. C. Cummins, *Inorg. Chem.* **2005**, *44*, 3127-3136.

[15] The formation of the dimer $(SPPPh_2NPPh_2S\text{-})_2$ has been conjectured to account for the formation of a Te(II) complex in the reaction of $TeCl_4$ and $HN(SPPh_2)_2$, but no experimental evidence was presented. J. Novosad, K. W. Törnroos, M. Necas, A. M. Z. Slawin, J. D. Woollins, S. Husebye, *Polyhedron*, **1999**, *18*, 2861-2867.

[16] D. C. Cupertino, R. W. Keyte, A. M. Z. Slawin, J. D. Woollins, *Polyhedron*, **1999**, *18*, 707-716.

[17] The ligand *t*Bu(Bu)P(S)NHP(S)P*t*Bu(Bu), in which the identity of the second Bu group on each P atom is not specified, has been mentioned briefly without details of the synthesis or spectroscopic characterization. P. Moore, W. Errington, S. P. Sangha, *Helvetica Chim. Acta*, **2005**, *88*, 782-795.

[18] V. L. Foss, Y. A. Veits, T. E. Chernykh, I. F. Lutsenko, *J. Gen. Chem. USSR (Engl. Transl.)* **1984**, *54*, 2386-2399.

[19] a) F. T. Fang, J. Najdzionek, K. L. Leneker, H. Wasserman, D. M. Braitsch, *Synth. React. Inorg. Met.-Org. Chem.* **1978**, *8*, 119-125; b) A. Schmidpeter, J. Ebeling, *Chem. Ber.* **1968**, *101*, 815-823; c) R. A. Shaw, E. H. M. Ibrahim, *Angew. Chem.* **1967**, *79*, 575-576; *Angew. Chem. Int. Ed. Engl.* **1967**, *6*, 556-556.

[20] J. Konu, T. Chivers, H. M. Tuononen, *Inorg. Chem.* **2006**, *45*, 10678-10687.

[21] D. Cupertino, R. Keyte, A. M. Z. Slawin, D. J. Williams, J. D. Woollins, *Inorg. Chem.* **1996**, *35*, 2695-2697.

[22] The S-S single bond length in *cyclo*-S_8 or MeS-SMe is 2.05 Å. Y. Steudel, M. W. Wong, R. Steudel, *Chem. Eur. J.* **2005**, *11*, 1281-1293.

[23] J. Jeske, A. Martens-Von Saizen, W-W. Du Mont, P. G. Jones, *Acta. Cryst*. **1998**, *C54*, 1873-1875.

[24] A. C. Hillier, S.-Y. Liu, A. Sella, M. R. J. Elsegood, *Angew. Chem.* **1999**, *111*, 2918-2920; *Angew. Chem. Int. Ed.* **1999**, *38*, 2745-2747.

[25] a) J. Jeske, W-W. du Mont, P. G. Jones, *Angew. Chem.* 1997, *109*, 2304-2306; Angew. Chem. *Int. Ed. Engl.* **1997**, *36*, 2219-2221; b) J. Jeske, W-W. du Mont, F. Ruthe, P. G. Jones, L. M. Mercuri, P. Deplano, Eur. J. *Inorg. Chem*. **2000**, 1591-1599.

[26] J. Konu, T. Chivers, H. M. Tuononen, *Chem. Commun*. **2006**, 1634-1636.

[27] A referee has suggested an alternative bonding description of **5c** in which a Te^{II} centre is chelated by two *anionic* ligands, (*Te,Te*)-$[(TeP{t}Bu_2)_2N]^-$ and (*P,Te*)-

[TeP*t*BuNP*t*Bu]$^-$. We note, however, that the sums of the calculated atomic charges for the two TePNPNTe units of **5c** are -0.53 and +0.53 and the calculated atomic charge for Te2, which would be the Te^{II} centre in the alternative bonding description, is +0.02. These values clearly support the view of **5c** as a "contact ion pair" with cationic and anionic halves of the molecule rather than the proposed Te^{II} complex.

[28] The planar eight-membered cyclic dication $[Et_4P_2N_4S_2]^{2+}$ also contains two-coordinate sulfur atoms, but the P(V) atoms are bonded to two N neighbours. M. Brock, T. Chivers, M. Parvez, R. Vollmerhaus, *Inorg. Chem*. **1997**, *36*, 485-489.

[29] The sum of van der Waals radii are as follows: two Te atoms (4.40 Å); Te and I (4.35 Å); S and I (4.00 Å). L. Pauling, *The Nature of the Chemical Bond*; 3rd Ed.; Cornell University Press; Ithaca, NY, **1960**, p. 260.

[30] C. Schade, W. Bauer, P. V. R. Schleyer, *J. Organomet. Chem.* **1985**, *295*, C25–C28.

[31] a) J. P. Perdew, K. Burke, M. Ernzerhof, *Phys. Rev. Lett.* **1996**, 77, 3865; b) J. P. Perdew, K. Burke, M.

Ernzerhof, *Phys. Rev. Lett*. **1997**, *78*, 1396; c) J. P. Perdew, K. Burke, M. Ernzerhof, *J. Chem. Phys.* **1996**, *105*, 9982; d) M. Ernzerhof, G. E. Scuseria, G. E. *J. Chem. Phys.* **1999**, *110*, 5029.

[32] A. Schäfer, C. Huber, R. Ahlrichs, *J. Chem. Phys.* **1994**, 5829-5835.

[33] All basis sets were used as they are referenced in the Turbomole 5.8 internal basis set library. TURBOMOLE, Program Package for *ab initio* Electronic Structure Calculations, Version 5.8. R. Ahlrichs, *et al.* Theoretical Chemistry Group, University of Karlsruhe, Karlsruhe, Germany, 2005.

[34] G. M. Sheldrick, SHELXL-97, Program for refinement of crystal structures, University of Göttingen, Germany, 1997.

Supporting Information

The 3D atomic coordinates for the optimized geometries of isomers **A** and **B** of $(EPR_2NPR_2E-)_2$ (E = S, Se, Te; R = *i*Pr, *t*Bu) are available as .mol2 files.

Figure Captions:

Figure 1. Thermal ellipsoid plot (30 % probability) of the structure of **5a.** The lattice THF molecules and all hydrogen atoms have been omitted for clarity.

Figure 2. Thermal ellipsoid plot (30 % probability) of the structure of **4b.** The lattice toluene molecule and all hydrogen atoms have been omitted for clarity.

Figure 3. Thermal ellipsoid plot (30 % probability) of the structure of **5b.** All hydrogen atoms have been omitted for clarity.

Figure 4. Thermal ellipsoid plot (30 % probability) of the structure of **5c.** All hydrogen atoms have been omitted for clarity.

Figure 5. A line drawing representation of the structure of **5c.**

Figure 6. The structure of **7a.** Hydrogen atoms have been omitted for clarity.

Figure 7. The structure of **7b** (E = Se) and **7c** (E = Te). Hydrogen atoms have been omitted for clarity.